Heat Treatment Optimization and Properties Correlation for H11-Type Hot-Work Tool Steel

B. PODGORNIK, G. PUŠ, B. ŽUŽEK, V. LESKOVŠEK, and M. GODEC

The aim of this research was to determine the effect of vacuum-heat-treatment process parameters on the material properties and their correlations for low-Si-content AISI H11-type hot-work tool steel using a single Circumferentially Notched and fatigue Pre-cracked Tensile Bar (CNPTB) test specimen. The work was also focused on the potential of the proposed approach for designing advanced tempering diagrams and optimizing the vacuum heat treatment and design of forming tools. The results show that the CNPTB specimen allows a simultaneous determination and correlation of multiple properties for hot-work tool steels, with the compression and bending strength both increasing with hardness, and the strain-hardening exponent and bending strain increasing with the fracture toughness. On the other hand, the best machinability and surface quality of the hardened hot-work tool steel are obtained for hardness values between 46 and 50 HRC and a fracture toughness below 60 MPa$\sqrt{m}$.

https://doi.org/10.1007/s11661-017-4430-1

I. INTRODUCTION

IN hot metal-forming applications, like forging, stamping, rolling, or die casting, the service life of the tool is limited by the extreme working conditions, including thermal, mechanical and impact loading, the high contact pressures, and the abrasive flow of the work material.[1,2] Under such complex working conditions, which may vary significantly across the tool, the tool surface is deteriorated and damaged through different wear mechanisms and thermo-mechanical fatigue processes.[3–5]

In recent years, the requirements for tool resistance and performance have become increasingly demanding, which is strongly related to tool design, material selection, and heat treatment optimization.[6] On one hand, an increase in energy costs,[7] the competitiveness of companies from emerging countries, and investments in new technologies dictate the increased productivity, efficiency, and performance of existing tools.[8] As die costs represent between 15 and 30 pct of the total costs of the forging process, producing more parts leads to a sizeable cost reduction and increased profitability.[1] Another major factor is coming from the automotive sector. The automotive industry is continuously working on reducing the weight of vehicles in order to lower fuel consumption and CO_2 emissions, while maintaining or even improving the strength of the components in accordance with increasing safety demands.[9] This requires the introduction of low-weight high-strength materials, which are very difficult and demanding to form.[10,11] A high-strength work material combined with the increased complexity of the formed parts results in tools working under extreme stresses.

Increased tool demands mean tougher property requirements for the tool material, including temper resistance, yield and ultimate tensile strengths, wear resistance, fatigue, and shock resistance, but mainly ductility and fracture toughness, which are essential for high-temperature forming applications.[12,13] The properties of tool steels depend on a balanced chemical composition and the processing route, but mainly on the heat treatment process, which defines the final microstructure. In general, the required properties, mainly the hardness and toughness are generated by a controlled heat treatment process consisting of an austenitization treatment with a subsequent hardening and a multiple tempering procedure.[12,14] Traditionally, a trade-off between high hardness and sufficient toughness is required, where the hardening and tempering parameters have to be chosen from a relatively narrow range.[15] On the other hand, through an optimized vacuum-heat-treatment procedure, a fine-grained microstructure with a homogeneous distribution of fine, secondary carbides and a reduced retained austenite content can be obtained,[13] thus satisfying ever greater demands on tool properties in terms of a greater fracture toughness and thermal fatigue resistance, while maintaining a high hardness and strength.[16]

B. PODGORNIK, G. PUŠ, B. ŽUŽEK, V. LESKOVŠEK, and M. GODEC are with the Institute of Metals and Technology, Lepi pot 11, 1000 Ljubljana, Slovenia. Contact e-mail: bojan.podgornik@imt.si
Manuscript submitted June 7, 2017.
Article published online December 12, 2017

The most common properties used for optimizing the heat treatment of tool steels are the hardness and the fracture toughness. A high hardness (46 to 50 HRC) is related to the resistance to plastic deformation and wear resistance, and the toughness to the tool's ability to resist crack initiation and propagation.[5,16] However, besides hardness and toughness there are also other tool-steel properties, which depending on the application are becoming important as we move towards increasingly complex tools. These include thermal conductivity, creep and wear resistance, compressive and bending strengths, as well as machinability.[11] Although different tool-steel properties can be determined using standard test methods, each one requires specific and often quite unique and demanding test specimens. Furthermore, the different geometries of standard specimens mean different heat treatment conditions, which result in microstructure deviations,[17] making it practically impossible to directly correlate the properties after a heat treatment. On the other hand, a circumferentially notched and fatigue-precracked tensile bar (CNPTB) specimen has been found to be the best alternative, which after a fracture toughness measurement can be used to determine many other properties.[18] The advantage of the CNPTB specimen lies in its radial symmetry, which makes the specimen particularly suitable for studying the influence of tool-steel properties and to optimize its heat treatment.[19]

The aim of this research work was to determine the effect of vacuum-heat-treatment conditions on different properties and their correlations for a low-Si-content AISI H11-type hot-work tool steel using a single CNPTB test specimen. Furthermore, this work is intended to show the potential of the CNPTB test specimen for property characterization, heat treatment optimization, and the design of forming tools.

II. EXPERIMENTAL

A. *Material and Heat Treatment*

The material used in the investigation was low-Si-content AISI H11-type hot-work tool steel with the following composition (wt pct): 0.36 pct C, 0.22 pct Si, 0.25 pct Mn, 5.02 pct Cr, 1.25 pct Mo, and 0.43 pct V. The material was delivered in the form of forged and soft-annealed blocks, from which the CNPTB specimens[18] (Figure 1) were machined in the short transverse direction.

The specimens were heat treated in an Ipsen VTC 324-R horizontal vacuum furnace with a uniform high-pressure gas-quenching system. The specimens were first preheated to 850 °C, followed by progressive heating at 10 °C/min to the austenitizing temperatures of 990 °C and 1030 °C. After soaking for 20 minutes, the specimens were quenched in N_2 gas at a quenching speed of 3 °C/s and double tempered for 2 hours. For each austenitizing temperature, the first tempering was performed at 540 °C, followed by a second tempering carried out at six different temperatures, varying between 550 °C and 630 °C. In terms of the vacuum-heat-treatment conditions employed (austenitizing and tempering temperatures), 12 sets of specimens, each

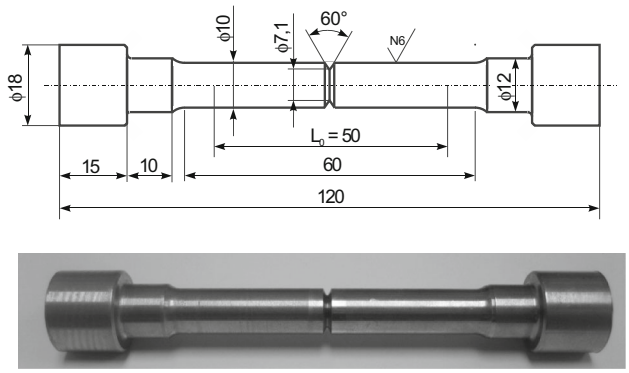

Fig. 1—CNPTB specimen.

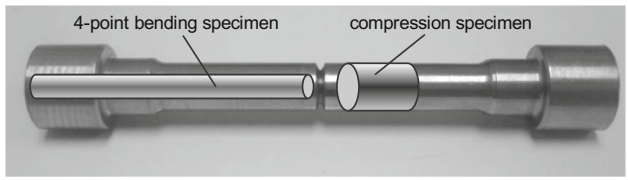

Fig. 2—Extraction of the 4-point bending and compression test specimens.

consisting of at least 12 samples were prepared in order to obtain statistically relevant results. After the heat treatment, the properties were evaluated, including fracture toughness, hardness, compression strength and strain-hardening exponent, bending strength, and machinability, with the results presented in the form of combined tempering diagrams.

B. *Properties Measurement*

Fracture toughness measurements were performed on non-standard CNPTB specimens,[18] with the fatigue pre-crack of about 0.5 mm created prior to the final heat treatment. The pre-cracking was done under a rotating bending loading of 400 N for 4500 cycles. As shown in Reference 20, the heat treatment has no negative effect on the crack-tip blunting and the measured fracture toughness values. After the heat treatment, the CNPTB specimens were subjected to tensile loading until fracture, using an Instron 1255 tensile-test machine, room temperature conditions, and a cross-head speed of 1.0 mm/min. By measuring the load at fracture (P), the diameter of the brittle fractured area (d) and knowing the size of the nominal non-notched specimen diameter (d_0 = 10 mm) the fracture toughness can be calculated using Eq. [1][21,22]:

$$K_{Ic} = \frac{P}{d_0^{3/2}} \cdot \left(-1.27 + 1.72\frac{d_0}{d}\right). \qquad [1]$$

The fracture toughness measurements were followed by measurements of the *Rockwell-C hardness*, carried out using a Wilson-Rockwell B2000 machine. The hardness measurements were performed circumferentially on both halves of each fractured CNPTB specimen and the average value was calculated.

From one half of the fractured CNPTB specimen, a ϕ 10 × 12.5 mm cylinder was cut for *compression testing* (Figure 2). The compression tests were carried out at room temperature using an Instron 1255 machine according to the ASTM E9-09 standard and a constant cross-head speed of 2.0 mm/min. The compression test results included the yield strength, maximum compression strength, and strain-hardening exponent, determined on a log–log plot of true-stress–true-strain between the yield and the maximum compression stresses. The other half of the fractured CNPTB specimen was used to machine a cylindrical *4-point bending test* specimen, with a diameter of 5 mm and a length of 60 mm (Figure 2). After machining with high-speed turning, the bending specimens were center-less ground in order to obtain the required surface roughness of 0.2 μm. Room-temperature 4-point bending tests were performed according to the ASTM E290-09 standard using the Instron 1255 machine and a cross-head speed of 2.0 mm/min. The support span was 40 mm and the load span was 16 mm. During testing, the maximum bending strength and the deformation at a load of 3.5 kN were determined.

Finally, the effect of heat treatment on the *machinability* of the hot-work tool steel was evaluated by analyzing the surface roughness of the 4-point bending specimens after the turning process. All the specimens were first pre-machined using Sandvik-Coromant DNMG11 R0.4 cutting inserts, a feed rate of 0.12 mm/rev, a depth of cut of 0.3 mm, and a cutting speed of 100 m/min. The final machining was done with VBMT 16 04 cutting inserts, a feed rate of 0.08 mm/rev, a depth of cut of 0.2 mm, and the same cutting speed of 100 m/min. For each specimen, new cutting inserts were used and the surface roughness was analyzed with an Alicona InfiniteFocus G4 system in terms of the R_a, R_z, R_p, R_v, R_{sk}, and R_{ku} roughness parameters, as defined in the ISO 4287 standard.

III. RESULTS

A. *Microstructure*

After quenching from 990 °C and double tempering, the microstructure of the investigated AISI H11-type hot-work tool steel consisted of some undissolved primary MC, M_6C, and $M_{23}C_6$-type carbides and very fine, Cr-rich M_7C_3 secondary carbides uniformly distributed in the matrix of fine, needle-like tempered martensite (Figure 3). The volume fraction of the primary carbides was ~ 2 pct. By increasing the austenitizing temperature to 1030 °C, a negligible fraction of bainite (< 1 pct) was observed, besides the typical microstructure of tempered martensite, as well as the pronounced dissolution of primary carbides in the austenitic matrix (Figure 4). The volume fraction of primary carbides was reduced to below 0.5 pct, with only V-rich MC carbides remaining, while other types were completely dissolved. Furthermore, higher austenitizing temperature also led to increased grain size and the martensitic lath size, as well as to the higher number of secondary carbides caused by increased quantity of solute atoms in the austenite prior to quenching.[23] An increased tempering temperature, on the other hand, resulted not only in a similar fine martensitic microstructure, but also in intensified precipitation[12] and up to 4 times more fine secondary carbides (Figures 3(b) and 4(b)). With the higher tempering temperature, also more pronounced precipitation of carbides along martensitic laths can be observed. The effect of the austenitizing and tempering temperatures on the number of secondary carbides as determined with a quantitative metallographic analysis performed using ImageJ software on 10 randomly selected SEI visible fields at 5000 times magnification is shown in Figure 5.

B. *Hardness and Fracture Toughness*

The tempering diagram showing the hardness and fracture toughness of the investigated AISI H11-type hot-work tool steel as a function of the austenitizing and tempering temperatures can be seen in Figure 6. The hardness obtained after quenching from 990 °C and double tempering at 630 °C was 40 HRC, and this increased to 49 HRC as the tempering temperature was reduced to 550 °C. The fracture toughness, on the other hand, dropped from 87 MPa$\sqrt{m}$ to less than 30 MPa$\sqrt{m}$. A further increase in hardness was obtained by increasing the austenitizing temperature, with a temperature of 1030 °C resulting in a hardness increase of about 5 pct and a maximum hardness of ~ 52 HRC. However, in

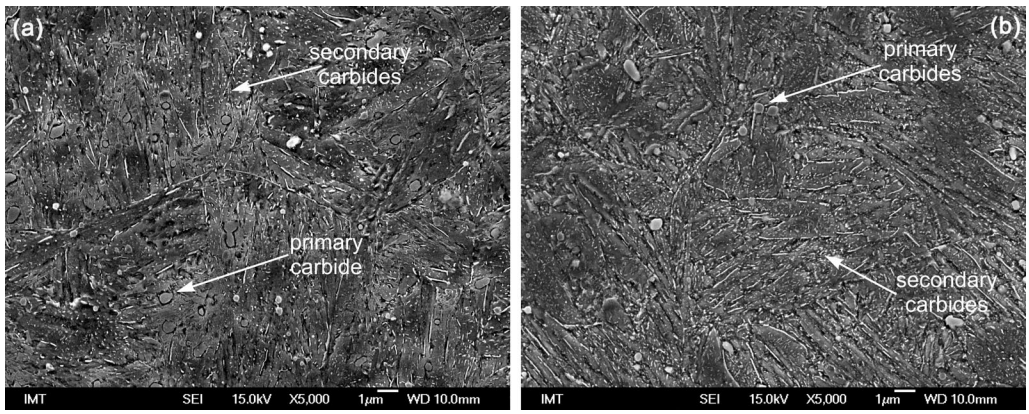

Fig. 3—Microstructure of quenched and tempered hot-work tool steel, quenched from 990 °C and tempered at (*a*) 550 °C and (*b*) 630 °C.

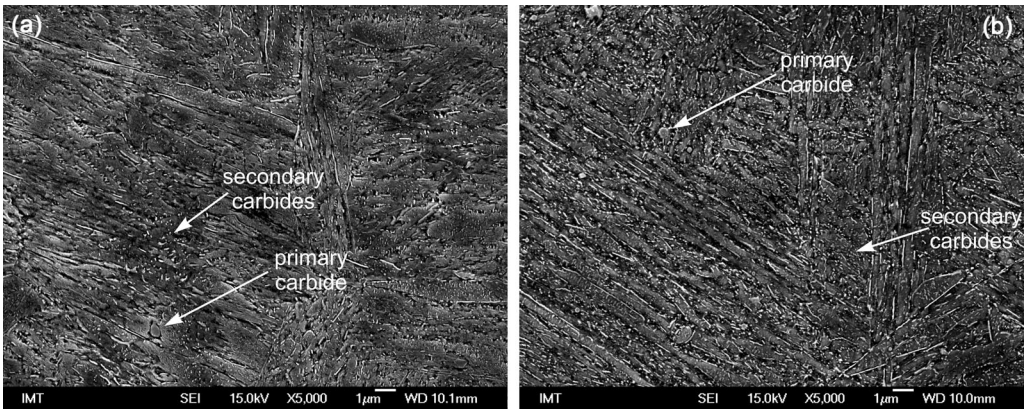

Fig. 4—Microstructure of quenched and tempered hot-work tool steel, quenched from 1030 °C and tempered at (*a*) 550 °C and (*b*) 630 °C.

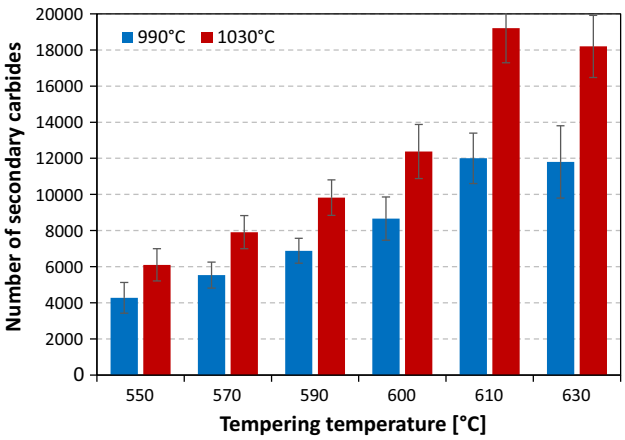

Fig. 5—Effect of the austenitizing and tempering temperatures on the number of secondary carbides.

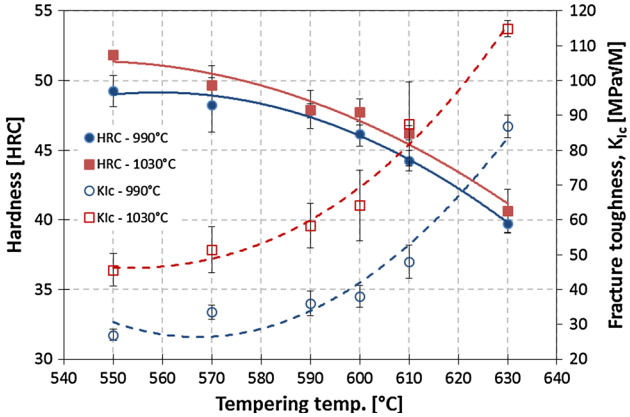

Fig. 6—Hardness and fracture toughness tempering diagram.

contrast to high-Si-content hot-work tool steels,[24] the higher austenitizing temperature also resulted in an elevated fracture toughness, ranging from 45 MPa√m even up to 115 MPa√m, as shown in Figure 6. Higher austenitizing temperature enhances dissolution of primary carbides and allows more carbide-forming elements to dissolve in the σ phase, which then precipitate during tempering in the form of small, nanometer-sized secondary carbides and result in an increased hardness. Almost complete dissolution of the coarser primary carbides also reduces the risk of voids creation around larger primary carbides due to plastic deformation,[23] thus simultaneously improving the hardness and fracture toughness. On the other hand, increasing the tempering temperature although leading to increased volume fraction of very fine secondary carbides also results in a reduction of the alloying elements content in the solid solution thus inducing a global softening of the tempered martensite but with the higher toughness.[25]

C. *Compression Test Results*

The yield and maximum compression strengths of the investigated hot-work tool steel range between 1200 and 1780, and 1450 and 2050, respectively. Analogously to the hardness, the yield and maximum compression strengths increase with the austenitizing temperature (by ~ 5 pct) as a consequence of a greater number of carbides being present in the microstructure, but decrease with the tempering temperature, as shown by the tempering diagram in Figure 7. During tempering, growth and dissolution combined with transition of different types of carbides and global softening of the tempered martensite take place,[23,25] resulting in a decreased strength of the material. In terms of the strain-hardening exponent, representing a measure of the material's ductility, it was found to be more-or-less independent of the heat treatment conditions. For the low and high austenitizing temperatures and tempering temperatures between 550 °C and 600 °C where martensite softening is compensated by an increased number of secondary carbides, the strain-hardening exponent shows a constant value of about 0.45. However, as the tempering temperature exceeded 610 °C, the strain-hardening exponent for the investigated hot-work tool steel increased to about 0.6 (Figure 7). As reported,[25] coalescence of carbides and the decrease of the density of dislocations above 600 °C to 610 °C will induce further softening of the material which then results in an increased strain-hardening exponent.

D. *Bending Strength*

In the case of the 4-point bending test, the yield and maximum strengths for the investigated steel quenched from 990 °C increased from 1860 and 3260 to 2600 and 4550 MPa, respectively, as the tempering temperature was lowered from 630 °C to 550 °C. By increasing the austenitizing temperature to 1030 °C, the yield and maximum bending strengths also increased, reaching peak values of 2700 and 4780 MPa at the tempering temperature of 550 °C (Figure 8). Like with the fracture toughness, the bending strain at the preset stress of 3500 MPa increased with the tempering temperature, especially at the temperatures above 600 °C, showing values between 3 and 10 pct. Furthermore, by increasing the austenitizing temperature, the resistance of the investigated steel to bending deformation was improved, with the deformation being reduced by about 20 pct, as shown in Figure 8. A synergistic effect of the increased hardness and the fracture toughness, obtained through increased precipitation of very fine secondary carbides is also manifested in an improved bending resistance.

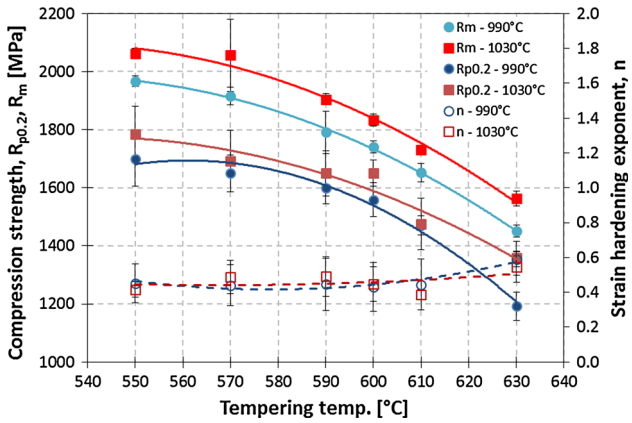

Fig. 7—Tempering diagram displaying compression test results.

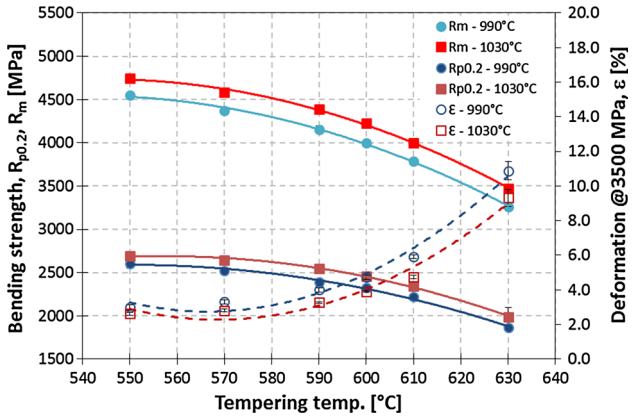

Fig. 8—Tempering diagram for 4-point bending test.

E. *Machinability*

The results of the surface-roughness measurements, performed on machined 4-point bending specimens to evaluate hot-work tool steel's machinability, are shown in Figure 9. Figure 9(a) shows the surface-roughness parameters, including the average surface roughness R_a, the maximum peak-to-valley height R_z, the maximum profile peak height R_p, and the maximum profile valley depth R_v. They all increase with an increased tempering, as well as the austenitizing temperature. This indicates an increased tearing component and worse machinability, caused mainly by an increased toughness and deformability of the material. For the machining conditions used and the applied austenitizing and tempering temperatures, the R_a value increased from 0.4 to 0.8 μm, and the R_z value from 2.5 to 4.5 μm (Figure 9(a)). Furthermore, the skewness (R_{sk}), being a measure of the surface profile asymmetry, was reduced with a higher tempering temperature from ~ 0 to − 0.5, and the

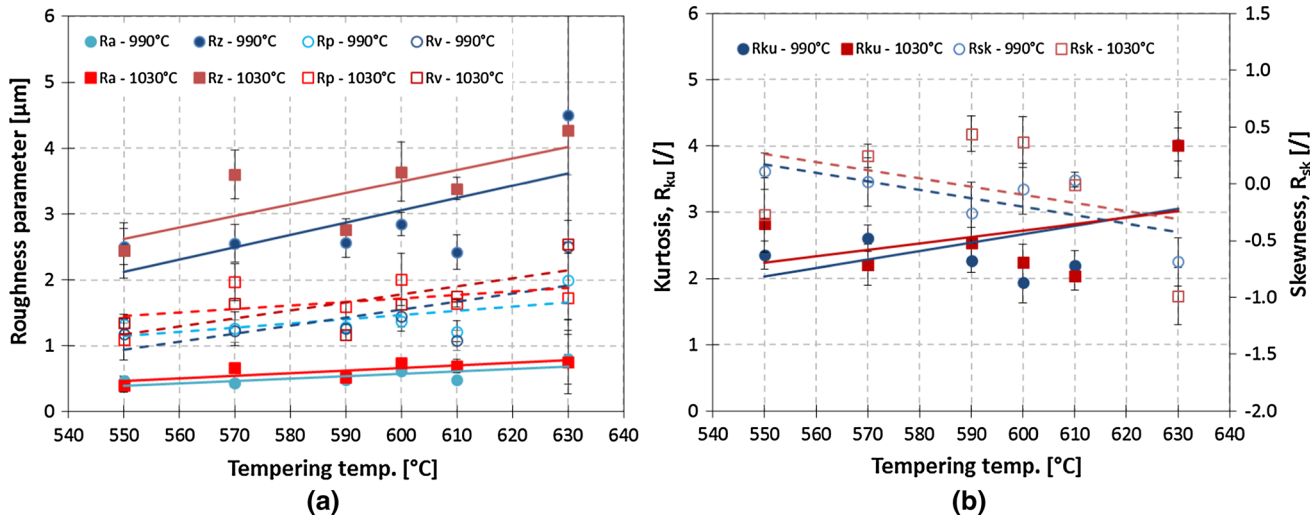

Fig. 9—Surface-roughness analysis of the machined hot-work tool steel; (*a*) standard roughness parameters, (*b*) kurtosis and skewness.

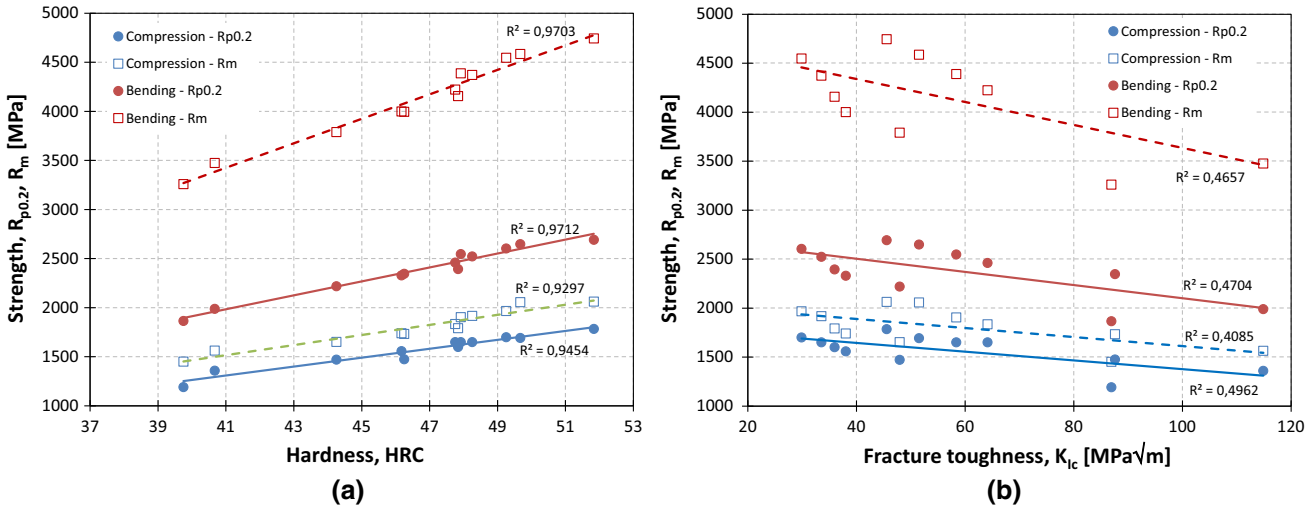

Fig. 10—Correlation between the compression and bending strengths and (*a*) the hardness and (*b*) the fracture toughness of the hot-work tool steel.

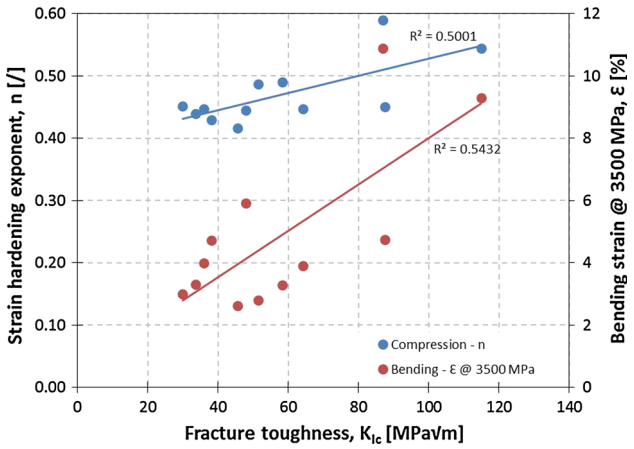

Fig. 11—Correlation between the fracture toughness and the strain-hardening exponent and the bending strain of the hot-work tool steel.

kurtosis (R_{ku}), displaying the sharpness of the surface profile increased from 2.5 to above 3. The austenitizing temperature, on the other hand, had only a marginal effect on the skewness and kurtosis values, as shown in Figure 9(b). A kurtosis above 3 characterizes the surfaces with sharp peaks and a negative skewness plateau-like topography.[26] As shown by the surface-roughness analysis, the machinability and the surface quality of the hot-work tool steel improved by lowering the tempering temperature and/or the austenitizing temperature (Figure 9) and increasing hardness.

IV. DISCUSSION

In the present case and for the heat treatment conditions applied, a strong correlation ($R^2 > 0.92$) between the investigated hot-work tool steel's hardness and the compression and bending strengths was observed. As shown in Figure 10, the compression and bending strengths increase linearly with the material's hardness and are reduced with the fracture toughness. Based on strong correlations, the yield and maximum compression strengths of the investigated hot-work tool steel can be expressed by hardness as 33.5 HRC and 38.6 HRC, respectively, and the bending yield and maximum stress as 51.0 HRC and 88.3 HRC, respectively. On the other hand, although the strain-hardening exponent and the bending strain show a correlation with the fracture toughness, both of them increasing with an improved fracture toughness of the material, the correlation factor R^2 is rather weak, being only about 0.5 (Figure 11).

In terms of surface quality and machinability, things are not so straight-forward. As shown in Figure 12(a), the roughness parameters (R_a, R_z, R_{sk}, R_{ku}), indicating improved machinability of the hot-work tool steel, improve with the increased hardness obtained through the increased austenitizing temperature and/or the reduced tempering temperature (Figure 6), resulting in an increased dissolution of the primary carbides and the martensite strengthening. However, if the material is too hard, above 50 HRC, the surface quality starts to deteriorate again, displaying sharp asperities and emphasized valleys. The same is true for the fracture toughness, with the surface quality and the machinability being deteriorated with the increased toughness of the material (Figure 12(b)). High toughness is an essential material characteristic for the hot-work tool steels, with brittle material absorbing less energy than a tough one before it fractures. Therefore, the higher the toughness of the material, the higher is the force needed to break it down. However, this also relates to the chip formation and material removal during machining. By reducing the hardness and increasing the toughness of the material to be machined, we are moving from cutting and chip breaking toward plastic deformation and material tearing and pull out within the cutting zone. Furthermore, materials with the higher toughness also show higher tendency to adhesion to the cutting tool and accelerated tool wear,[27] thus resulting in poor

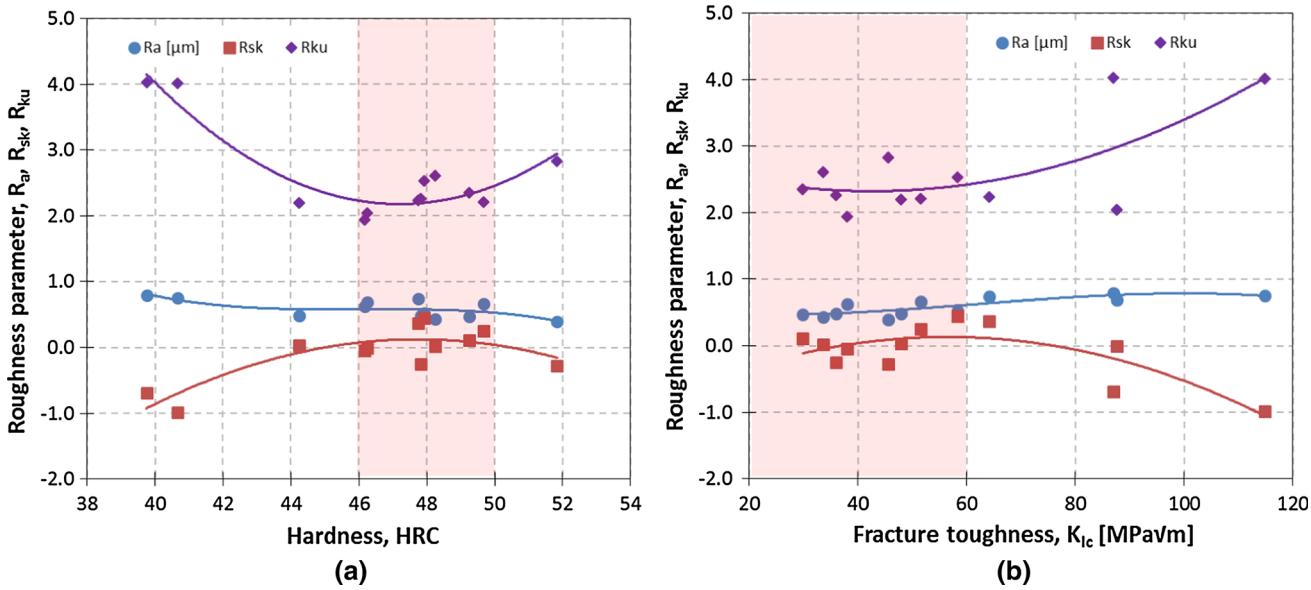

Fig. 12—Effect of (*a*) hardness and (*b*) fracture toughness on the surface roughness and quality.

quality of the machined surface. However, when material becomes too hard it accelerates tool wear and loss of cutting edge sharpness, again resulting in material deformation and pull out rather than in material cutting. In general, for the investigated AISI H11-type hot-work tool steel, the best machinability and surface quality are obtained when the material hardness is between 46 and 50 HRC and the fracture toughness is below 60 MPa√m, as shown in Figure 12.

V. CONCLUSIONS

The results of the research work performed can be summarized with the following conclusions:

1. A CNPTB specimen allows a simultaneous determination and correlation for multiple properties of hot-work tool steels, including the hardness, the compression and bending strengths, the fracture toughness and the strain-hardening exponent, the wear resistance and the machinability, which can all be directly correlated with the microstructure and used to design advanced tempering diagrams.
2. In the case of AISI H11-type hot-work tool steel with a low Si content, the hardness, the strength, and the fracture toughness increase with a higher austenitizing temperature, providing increased dissolution of primary carbides and intensified precipitation. On the other hand, the hardness and strength are reduced with tempering temperature, which although leading to increased volume fraction of secondary carbides results in the reduction of the alloying elements content in the solid solution and global softening of the material.
3. The yield and maximum compression and bending strengths show direct and very strong correlations with the increased hardness and reduced fracture toughness. Also the strain-hardening exponent and the bending strain increase with fracture toughness, although the correlation is rather weak.
4. The surface quality and the machinability of the heat-treated hot-work tool steel strongly depend not only on the hardness, but also on the fracture toughness, with the increased toughness leading to pronounced plastic deformation and tearing of the material. The best results are obtained when the hardness is between 46 and 50 HRC and the fracture toughness is below 60 MPa√m.

ACKNOWLEDGMENT

This work is part of the research programs P2-0050 and P2-0231, which are financed by the Slovenian Research Agency.

REFERENCES

1. M. Pérez and F.J. Belzunce: *Mater. Sci. Eng., A*, 2015, vol. 624, pp. 32–40.
2. B. Podgornik, V. Leskovšek, F. Tehovnik, and J. Burja: *Surf. Coat. Technol.*, 2015, vol. 261, pp. 253–61.
3. D. Mellouli, N. Haddar, A. Köster, and H.F. Ayedi: *Eng. Fail. Anal.*, 2014, vol. 45, pp. 85–95.
4. S. Malm and L.A. Norström: *Metal Sci.*, 1979, vol. 9, pp. 544–50.
5. V. Leskovšek, B. Šuštaršič, and G. Jutriša: *J. Mater. Process. Technol.*, 2006, vol. 178, pp. 328–34.
6. *Tool Steels*, 5th ed., G. Roberts, and G. Krauss, and R. Kennedy, eds., *Tool Steels*, 5th ed., ASM International, Materials Park, OH, 1998.
7. Euroforge.org: *2014 Energy cost/ratios in the European forging industry,* 2015. http://www.euroforge.org/fileadmin/user_upload/Downloads/Energy_Euroforge.pdf Accessed 26 May 2017.
8. M. Shirgaokar: *Technology to Improve Competitiveness in Warm and Hot Forging -Increasing Die Life and Material Utilization*, Ph.D. Dissertation, Ohio State University, Columbus, OH, 2008.

9. T.K. Ellera, L. Greve, M. Andres, M. Medricky, V.T. Meinders, and A.H. van den Boogaard: *J. Mater. Process. Technol.*, 2016, vol. 228, pp. 43–58.
10. B.A. Behrens, E. Doege, S. Reinsch, K. Telkamp, H. Daehndel, and A. Specker: *J. Mater. Process. Technol.*, 2007, vol. 185, pp. 139–46.
11. B. Podgornik and V. Leskovšek: *Steel Res. Int.*, 2013, vol. 84, pp. 1294–1301.
12. A. Eser, C. Broeckmann, and C. Simsir: *Comput. Mater. Sci.*, 2016, vol. 113, pp. 280–91.
13. J.-Y. Li, Y.-L. Chen, and J.-H. Huo: *Mater. Sci. Eng. A*, 2015, vol. 640, pp. 16–23.
14. M. Ramezani, T. Pasang, Z. Chen, T. Neitzert, and D. Au: *J. Mater. Res. Technol*, 2015, vol. 4, pp. 114–25.
15. C. Lerchbacher, S. Zinner, and H. Leitner: *Mater. Sci. Eng., A*, 2013, vol. 564, pp. 163–68.
16. G. Telasang, J. Dutta Majumdar, G. Padmanabham, and I. Manna: *Mater. Sci. Eng. A*, 2014, vol. 599, pp. 255–67.
17. J.L. Dossett and G.E. Totten: *ASM Handbook Volume 4A: Steel Heat Treating Fundamental and Processes*, ASM International, Materials Park, OH, 1991.
18. B. Podgornik, B. Žužek, and V. Leskovšek: *Mater. Perfor. Charact.*, 2014, vol. 3, pp. 1–9.
19. V. Leskovsek, B. Ule, and A. Rodic: *Metall. Alloys Technol.*, 1993, vol. 27, pp. 195–204.
20. B. Ule, V. Leskovsek, and B. Tuma: *Eng. Fract. Mech.*, 2000, vol. 65, pp. 559–72.
21. S. Wei, Z. Tingshi, G. Daxing, L. Dunkang, L. Poliang, and Q. Xiaoyun: *Eng. Fract. Mech.*, 1982, vol. 16, pp. 69–82.
22. E.E. Gdoutos: *Fracture Mechanics Criteria and Applications*, Kluwer Academic Publishers, London, 1990.
23. I. Souki, D. Delagnes, and P. Lours: *Proc. Eng.*, 2011, vol. 10, pp. 631–37.
24. R.A. Mesquita, C.A. Barbosa, E.V. Morales, and H.-J. Kestenbach: *Metall. Mater. Trans. A*, 2011, vol. 42A, pp. 461–72.
25. N. Mebarki, D. Delagnes, P. Lamesle, F. Delmas, and C. Levaillant: *Mater. Sci. Eng. A*, 2004, vols. 387–389, pp. 171–75.
26. M. Sedlaček, B. Podgornik, and J. Vižintin: *Tribol. Int.*, 2012, vol. 48, pp. 102–12.
27. N. Sandberg: On the Machinability of High Performance Tool Steels, Ph.D. Thesis, Uppsala University, 2012.